Científica

vol. 30, no. 1, January-June 2026, pp. 01-12
ISSN 2594-2921, Instituto Politécnico Nacional, MÉXICO
e300105 | DOI: 10.46842/ipn.cien.v30n1a05

This article is featured in the Special Issue on TRIBOLOGY

Effect of high temperature on hardness and abrasive resistance of AISI 304 austenitic stainless steel

Efecto de la alta temperatura en la dureza y la resistencia a la abrasión del acero inoxidable austenítico AISI 304

Josué O. **Arreola Vargas**
Universidad de Guadalajara | MÉXICO

María E. **Sedano Hernández**
Universidad de Guadalajara | MÉXICO

Sara I. **Topete Velasco**
Universidad de Guadalajara | MÉXICO

Francisco J. **Aranda García**
Universidad de Guadalajara | MÉXICO

César **Sedano de la Rosa**
Universidad de Guadalajara | MÉXICO

https://científica.site

Recibido 15/04/2026, aceptado 28/05/2026.

Científica

vol. 30, no. 1, January-June 2026, pp. 01-12
ISSN 2594-2921, Instituto Politécnico Nacional, MÉXICO
e300105 | DOI: 10.46842/ipn.cien.v30n1a05

ARTICLE

Effect of high temperature on hardness and abrasive resistance of AISI 304 austenitic stainless steel

Efecto de la alta temperatura en la dureza y la resistencia a la abrasión del acero inoxidable austenítico AISI 304

Josué O. **Arreola Vargas** [1]
María E. **Sedano Hernández** [2]
Sara I. **Topete Velasco** [3]
Francisco J. **Aranda García** [4]
César **Sedano de la Rosa** [5]

Universidad de Guadalajara,
Departamento de Ingenierías,
Centro Universitario de la Costa Sur,
Autlán de Navarro, MÉXICO

[1] ORCID: 0009-0004-3457-8756 / josuearreola1206@gmail.com
[2] ORCID: 0000-0003-1677-6658 / sedano.hdez@gmail.com
[3] ORCID: 0009-0003-7346-6004 / sara.topete@academicos.udg.mx
[4] ORCID: 0000-0002-3708-9761 / francisco.aranda@academicos.udg.mx
[5] ORCID: 0000-0002-8684-8664 / cesar.sedano@academicos.udg.mx

Recibido 15/04/2026, aceptado 25/05/2026.

Abstract

Abrasive wear is a very common type of wear, and at the same time quite serious. It manifests itself when two surfaces in direct physical contact interact, and one is significantly harder than the other. In the present study, the abrasive wear resistance of AISI 304 austenitic stainless steel was evaluated using a dry abrasion test bench. The process of characterization of the wear scars was carried out using the scanning electron microscopy (SEM) and contact profilometry. In addition, hardness measurements were made to specimens before and after each test. The samples were made of austenitic stainless steel AISI 304. Abrasive silica sand particles (SIO_2) were sieved, and the particles retained in mesh 60 (250 to 297 µm) were used. The rated glide speed was 200 RPM and a slip distance of 4,309 m. The tests were performed at three different temperatures: 23 °C, 200 °C, and 400°C, and at 45 N. The loss of mass was monitored every 1,000 m of slippage and with the data obtained the wear rates and wear coefficients were calculated. Gravimetric results showed that the wear rate decreases with increasing temperature, slight increase in hardness was observed on the surface of the specimens as the temperature increases in the tests. Some wear mechanisms were identified at different temperatures such as plastic deformation, indentations, and plowing action mainly. Finally, higher wear rates were observed as the temperature increased, concluding that high temperatures promote an increase in the wear rate.

Index terms: dry abrasion, silica sand, austenite, stainless steel, high temperature.

Resumen

El desgaste abrasivo es un tipo de desgaste muy común y, a la vez, bastante grave. Se manifiesta cuando dos superficies en contacto físico directo interactúan, siendo una significativamente más dura que la otra. En el presente estudio, se evaluó la resistencia al desgaste abrasivo del acero inoxidable austenítico AISI 304 mediante un banco de ensayos de abrasión en seco. La caracterización de las huellas de desgaste se realizó mediante las técnicas de microscopía electrónica de barrido (SEM) y perfilometría de contacto. Además, se midió la dureza de las muestras antes y después de cada ensayo. Las muestras se fabricaron con acero inoxidable austenítico AISI 304. Las partículas de arena de sílice abrasiva (SiO_2) fueron tamizadas y se utilizaron las retenidas en la malla No. 60 (250 a 297 µm). La velocidad de deslizamiento nominal fue de 200 RPM y la distancia de deslizamiento de 4,309 m. Las pruebas se realizaron a tres temperaturas: 23°C, 200°C y 400°C, y a 45 N. La pérdida de masa se monitoreó cada 1,000 m de deslizamiento y, con los datos obtenidos, se calcularon las tasas y los coeficientes de desgaste. Los resultados gravimétricos mostraron que la tasa de desgaste disminuye con el incremento de la temperatura, se observó un ligero aumento en la dureza en la superficie de los especímenes conforme se incrementó la temperatura durante los ensayos. Además, se identificaron algunos mecanismos de desgaste a diferentes temperaturas, como deformación plástica, indentaciones y arado, principalmente. Finalmente, se observaron mayores tasas de desgaste a medida que aumentaba la temperatura, lo que permitió concluir que las altas temperaturas promueven un aumento de la tasa de desgaste.

Palabras clave: abrasión seca, arena de sílice, austenita, acero inoxidable, alta temperatura.

I. Introduction

The microstructure of steels is strongly affected by temperature due to their allotropic properties, and it is well established that steels begin to lose mechanical strength and elasticity appreciably between 315 and 370°C [1]. Abrasive wear, particularly under elevated temperatures, is a critical degradation mechanism in metallic materials, where parameters such as normal load and sliding velocity play decisive roles in determining wear rates and surface damage [2]. To evaluate these processes, standardized dry abrasion tests such as ASTM G65 are widely employed, using block-on-disk or sand/rubber wheel configurations [3]. These methods allow the study of sliding wear without lubrication, considering the inevitable formation of oxide layers and atmospheric contaminants on metallic surfaces. Previous investigations, have developed high-temperature abrasive wear benches capable of reaching 1000 °C. Their results demonstrated that the highest wear rates occurred at 900°C, confirming that elevated temperatures accelerate material loss [4]. Recent research has confirmed that temperature and load are decisive factors in the tribological behavior of stainless steels. Zhou et al. [5] observed that the wear of 304L intensifies between 25 and 400°C, with a shift in the mechanisms toward adhesive-oxidative processes. Similarly, Karabeyoğlu et al. [6] reported that the wear of 304L transitions from adhesive to abrasive as the temperature increases up to 200 °C. Finally, Ahmed and Mulapeer [7] compared the performance of austenitic and duplex steels, showing that 304 exhibits higher wear rates under high-temperature conditions, highlighting the need to evaluate its strength in critical applications. In this context, the present study aims to assess the abrasive wear behavior of AISI 304 stainless steel at room temperature, 200°C, and 400°C, employing a dry abrasion test bench to provide insights into the performance of widely used austenitic steels under severe operating conditions.

II. Experimental setup

A. Experimental test rig

The sample holder was fabricated from 7075 aluminum alloy, a lightweight material with high mechanical strength and a melting point of approximately 483°C. This alloy is widely used in injection molds, thermoforming applications, mechanical components, and aerospace structures [8]. To integrate the mechanical redesign of the sample holder into the tribometer and enable high-temperature testing, the following components were used: an XM TE96 temperature controller with a range of 50-450°C, powered by 220 V AC; a ManHua M1A4825A solid-state relay; a pair of 400 W, 220 V cartridge resistors; and a J2M temperature sensor (see Figure 1). Additionally, a 20 kg cantilever load cell was used to measure the load applied to the system.

A set of specifications was also formulated to differentiate the details of operation and those of design considering some parameters of the ASTM G-65 standard. The materials used in the re-design were selected considering the temperatures handled inside the test chamber. Subsequently, to complete the construction stage of the redesigned arm and the sample holder, it was necessary to make use of the equipment of the laboratories of Machines-Tools and Welding of CUCSUR. Once the load application arm has been modified and the machining of the sample holder completed, the samples were assembled into the equipment and then the components of the heating system were connected. To do this, two cartridge-type biphasic resistors were installed in the machined cavities inside the sample holder, connecting one phase with the solid-state relay and the other to the thermo-magnetic switch of the load center. In turn the solid-state relay was connected to the terminals of the temperature controller, a solid-state relay was also used instead of an electromechanical relay (contactor) because solid state relays do not have moving parts for their operation, and therefore they do not present a wear in the electrical components since their operation is based entirely on semiconductor electronics. Finally, a temperature sensor (thermocouple) was also connected to the controller to monitor the temperature of the sample.

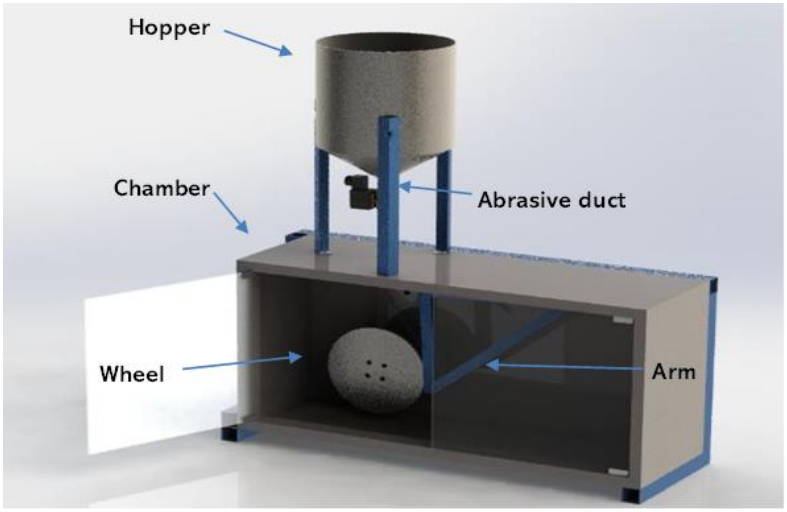

Fig. 1. Schematic diagram of abrasive test bench.

B. Materials and test process

The abrasive material used in the experiments was silica sand obtained from a local deposit in Casimiro Castillo, Jalisco. This sand is composed mainly of quartz (SiO_2), the second most common mineral in the earth's crust and is usually found in isolation or in symmetrical groupings of identical crystals (twinned) and in hexagonal crystals with trigonal pyramid termination, which can reach considerable sizes. It is a very resistant mineral, with hardness 7 on the Mohs scale, according to its color it is classified into a wide variety of subtypes, macrocrystalline (rock crystal, milky quartz, rose quartz, amethyst, citrine, smoky quartz) and cryptocrystalline (chalcedony) [9].

To carry out experiments a special particle size was used, and for this purpose a process of separation of particles was carried out by means of a sieving machine (Alcon brand). For this process, a sieve arrangement with meshes 30, 40, 50, 60 and 80 were used. The particles used in the tests were those that crossed mesh 50 and were retained in mesh 60, that is, they have a size ranging from 250 to 297 μm and have an irregular geometric shape, as shown in Figure 2.

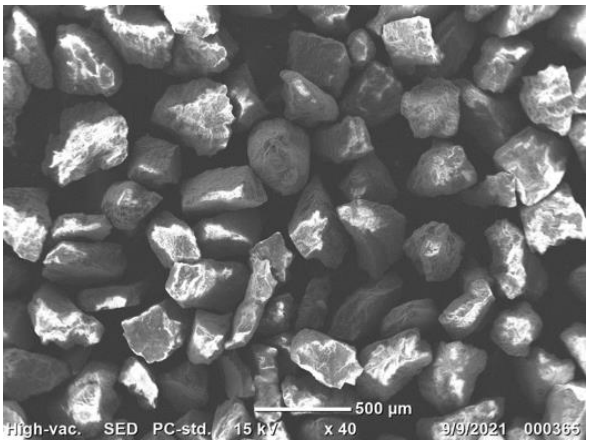

Fig. 2. Micrograph of abrasive particles.

AISI 304 austenitic stainless steel specimens were cutted out with dimensions of 20 × 60 mm and a thickness of 3.2 mm. This steel contains between 18–20% Cr and 8–10.5% Ni as its main alloying elements. It exhibits lower electrical and thermal conductivity than carbon steel, low magnetization, and high corrosion resistance, making it a widely used material in industrial applications. Its composition was developed by Hatfield at Firth-Vickers in 1924 and marketed under the name "StayBrite 18/8" [10].

The experimental setup was carried out following the parameters of ASTM G-65. The disc speed was set at 200 rpm and the total sliding distance at 4000 m. The tests were carried out at three temperatures 23, 200 and 400°C and a load of 45 N. The test parameters are summarized in Table 1. Mass loss was monitored every 1,000 m of sliding using a BOECO model BAS-31 plus analytical balance, with a precision of 0.1 mg.

TABLE 1
TEST CONDITIONS FOR DRY ABRASION EXPERIMENTS

Test conditions	Value
Temperature (°C)	23, 200 and 400
Applied load (N)	45
Sliding distance (m)	1,000, 2,000, 3,000 and 4,000
Mass Flow of abrasive material (g/min)	169
Disk speed (rpm)	200

III. RESULTS AND DISCUSSION

Once the preliminary tests were carried out to verify the proper functioning of the adapted systems in the equipment, the abrasive wear resistance on austenitic stainless steel AISI 304 was evaluated. The tests were performed at three temperatures: 23, 200 and 400°C, and a load of 45 N. The loss of mass was monitored every 1,000 m of slippage and with the data obtained the corresponding wear rates were calculated.

In Figure 3a the traces of wear obtained for the maximum sliding distance (4000 m) are observed, on the left side of the image the specimen tested at room temperature is shown, in the central part that corresponding to 200°C and to the right that of 400°C, in the latter a darker hue than the previous two samples is observed with the naked eye, indicating that at 400°C oxidation is promoted on the surface of the samples. Figure 3b shows a cross-sectional of the sample tested at 400°C where the aforementioned oxidation layer is observed.

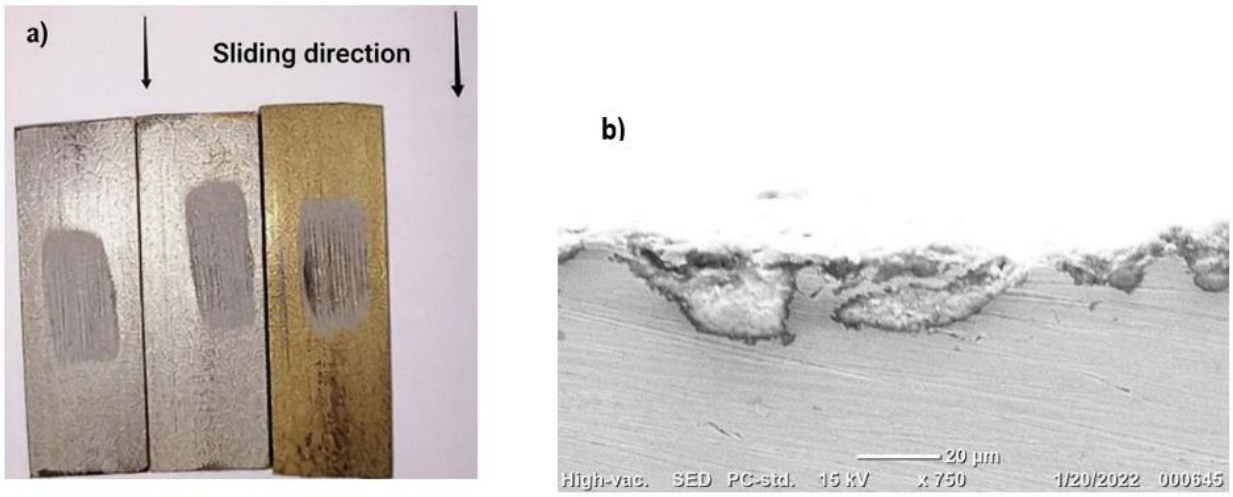

Fig. 3. a) Traces of wear on stainless steel specimens at room temperature, 200 and 400°C, from left to right, respectively; b) Micrograph of the cross section of the stainless steel sample tested at 400°C.

The wear scar in the samples was monitored gravimetrically every 1000 m of sliding, derived from these measurements in Figure 4 presents the wear rate in relation to temperature for different sliding distances. Where it can be observed that as the temperature is increased in abrasion tests, the wear rate decreases. This phenomenon can be explained by the softening of stainless steel due to the heat emitted by the heating elements, thus producing many plastic deformations and eventually a low detachment of the deformed material. In the same figure a similar behavior is also observed in the tests at room temperature and at 200°C, while in the tests at 400°C the graph shows a different behavior. This indicates that at this temperature the mechanisms of material release are different from the other two lower temperatures. On the other hand, in figure 5 the wear coefficient obtained is observed, which presents its highest value at room temperature and, on the contrary, the lowest value was observed at 400°C, it should be noted that these results are consistent with the behavior of wear rates.

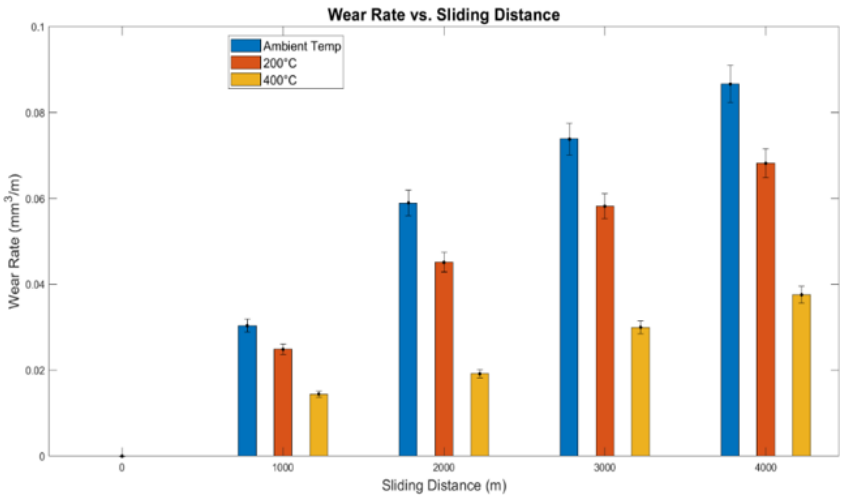

Fig. 4. Wear rate at different sliding distances.

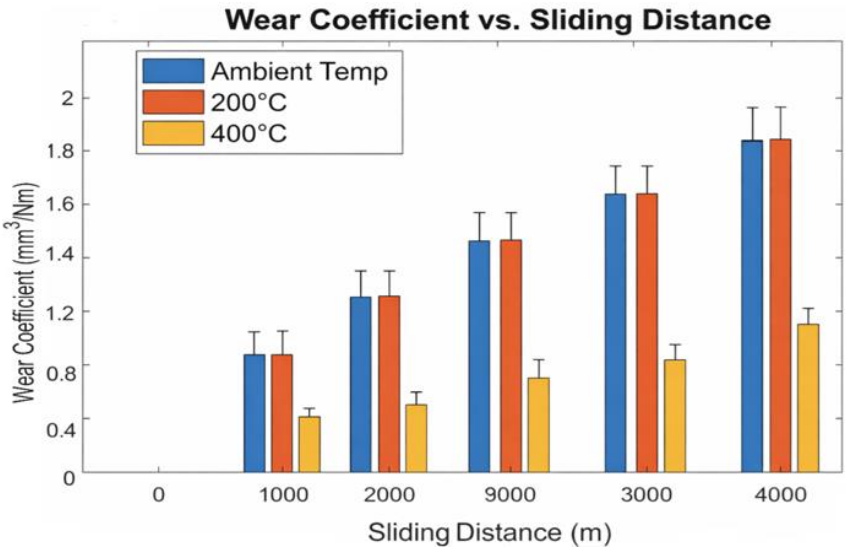

Fig. 5. Wear coefficient sliding distance.

A. Wear mechanisms

Figure 6a shows the plowing action obtained at 4000 m slippage and 200°C. On the other hand, figure 6b shows the plowing action under the same test conditions increasing the temperature to 400°C. In both micrographs it is clearly seen how temperature affects the number and shape of the grooves generated on the surface of the specimens. In the first figure, which was tested at a lower temperature, the grooves are observed with a lower definition. While in the second, subjected to 400°C, the grooves are observed with greater definition. This may be possible because stainless steel softens at a higher temperature making it more ductile, in this way the higher the temperature the greater the plastic deformation in the material. Finally, the wear mechanisms observed during the dry abrasion tests at high temperatures were predominantly plastic deformation and plowing action, as can be seen in Figure 6c. In the meantime, in Figure 6d there are indentations of silica sand particles on the surface of austenitic stainless steel which promotes the appearance of cracks.

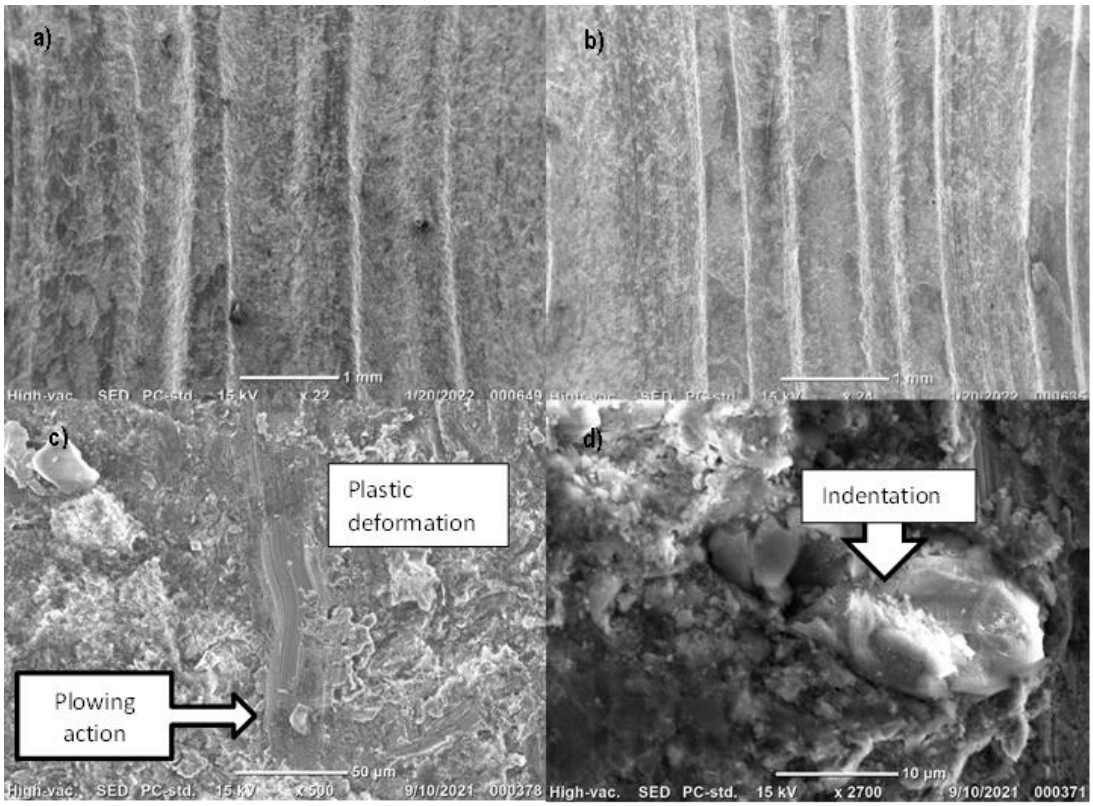

Fig. 6. Micrographs with a) Plowing action on the sample at 200°C. b) Plowing action on the sample at 400°C. (c) Wear track after 4000 m of sliding at 200 °C d) Particle embedded at 4000 m slide at 400°C.

After the abrasion tests at high temperatures, the hardness was measured in three different areas of each sample using a portable hardness tester. With the results obtained, the graph shown in Figure 7 was constructed, where a slight increase in hardness is observed on the surface of the specimens as the temperature increases in the tests; that is, the samples probably soften during the tests and after, with the cooling of the sample, they acquire a greater hardness due to the thermal effect induced during the tests.

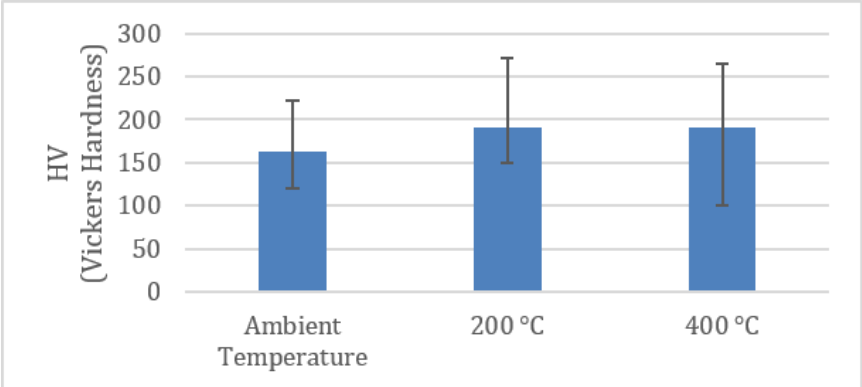

Fig. 7. Surface hardness plot of samples after testing.

Científica, vol. 30, no. 1, pp. 01-12, January-June 2026,
ISSN 2594-2921, Instituto Politécnico Nacional, México
e300105 | DOI: 10.46842/ipn.cien.v30n1a05

The profilometry results confirm that increased temperature reduces the depth and severity of wear, although it increases plastic deformation. Figure 8a shows a pronounced central depression, with depths close to -300 µm, indicating severe wear dominated by fracture and particle removal. The profile shown in Figure 8b exhibits less abrupt variations, with maximum depths around -250 µm, reflecting a more widespread but shallower indentation. This behavior suggests a predominance of plastic deformation with less material removal. Figure 8c shows oscillations between -250 µm and -100 µm, with a tendency to recover to near-zero levels towards the end of the measurement. The result indicates less severe wear in terms of mass loss, although with greater surface deformation, attributable to the thermal softening of the stainless steel.

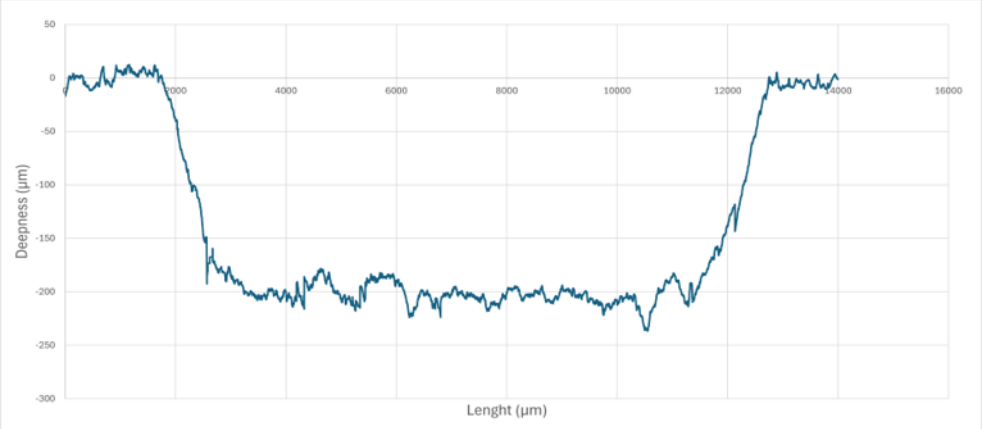

Fig. 8a. Profilometry of specimen tested at room temperature.

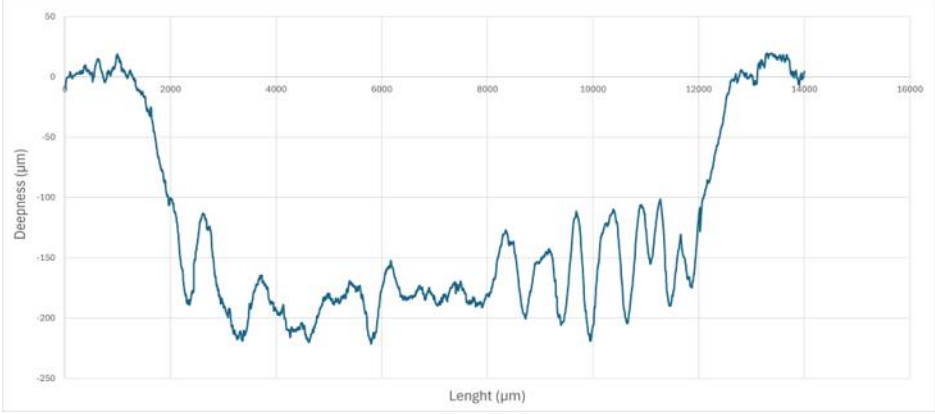

Fig. 8b. Profilometry of specimen tested at 200°C.

Científica, vol. 30, no. 1, pp. 01-12, January-June 2026,
ISSN 2594-2921, Instituto Politécnico Nacional, México
e300105 | DOI: 10.46842/ipn.cien.v30n1a05

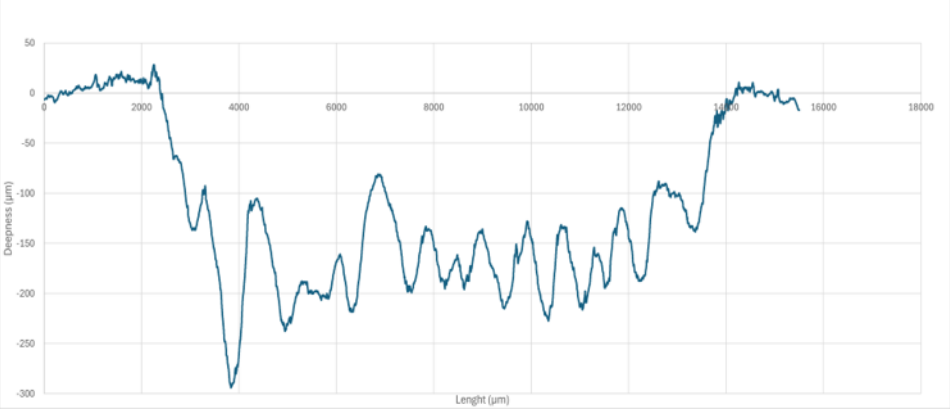

Fig. 8c. Profilometry of specimen tested at 400°C.

B. Raman spectroscopy analysis

The graph illustrates the evolution of the chemical phases present on the surface of the AISI 304 stainless steel subjected to abrasive wear, revealing a clear dependence of oxide film formation on the testing temperature.

Room Temperature (RT - Black line), the spectrum is essentially flat, without well-defined Raman scattering peaks. This indicates the absence of a thick or crystalline oxide layer. During wear at RT, the mechanical removal of material dominates over any oxidation kinetics. The natural passive layer of stainless steel is thin (nanometric scale) to generate a strong Raman signal; therefore, the exposed surface corresponds primarily to the freshly plastically deformed metallic matrix.

At 200°C (Red line), slight changes begin to appear. A minor increase in the background signal and the development of broad, low-intensity bands (mainly in the 500-700 cm^{-1} region) are observed. This evidences the onset of an incipient tribo-oxidation process. However, the lack of sharp peaks suggests that the formed oxides are amorphous, very thin, or lack long-range crystalline order due to the continuous mechanical disruption from abrasive wear.

At 400°C (Blue line), the spectrum exhibits a drastic change in surface chemistry, revealing intense and well-defined peaks that confirm a regime of severe tribo-oxidation. The most prominent peak is located around 670-680 cm^{-1}. This is the classic spectroscopic signature of magnetite (Fe_3O_4) and iron-chromium rich spinel-type oxides ($FeCr_2O_4$). This phase is completely consistent with the dark coloration macroscopically observed on the wear track.

The lower intensity peaks in the 300-400 cm^{-1} region and near 550 cm^{-1} typically correspond to the coexistence of other iron oxide phases (such as hematite Fe_2O_3) and chromium oxide (Cr_2O_3), formed by the preferential oxidation of alloying elements at this elevated temperature.

The broad bands observed above 1300 cm^{-1} are usually attributed to second-order scattering or structural defects in the oxide lattice induced by the severe mechanical deformation and friction.

A direct comparison between the Raman spectra obtained inside and outside the wear track isolates the effect of frictional heating from the ambient testing temperature. At RT and 200°C, both regions exhibit essentially flat spectra, indicating that neither ambient heat nor frictional energy is sufficient to promote significant oxide growth; thus, severe

metallic wear prevails. However, a critical contrast is observed at 400°C. While the spectrum outside the wear track shows the onset of thermal oxidation with low-intensity peaks, the spectrum inside the track at the same temperature displays highly intense, sharp, and well-defined peaks corresponding to magnetite and iron-chromium spinels (centered at ~670 cm^{-1}). This stark difference in peak intensity and definition provides conclusive evidence that the protective dark layer is a tribochemical product. It is the synergistic combination of the high ambient temperature (400°C), localized frictional flash temperatures, and severe plastic deformation that provides the necessary activation energy to accelerate the oxidation kinetics. This mechanism leads to the formation of a thick, highly crystalline protective tribo-layer (glaze layer) inside the wear scar, which acts as a solid lubricant and is fundamentally responsible for the minimization of the wear coefficient at high temperatures (see Fig. 9).

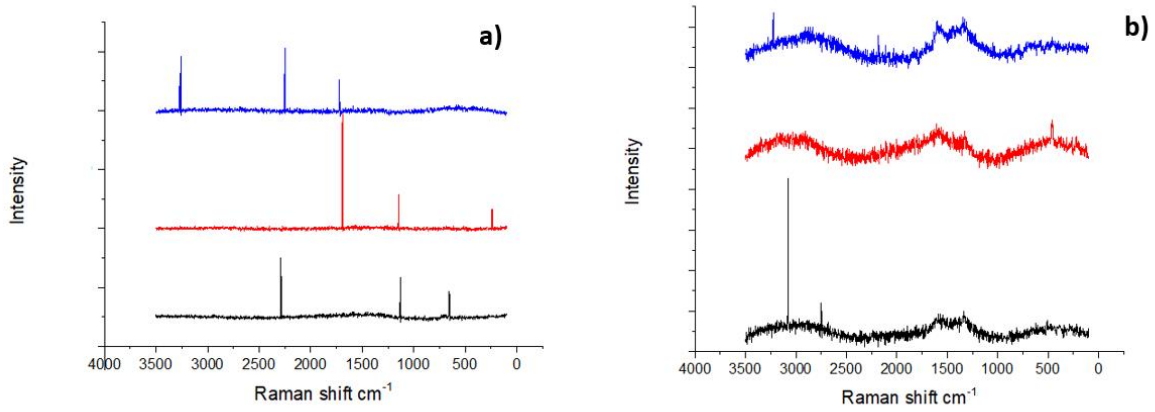

Fig. 9. Raman spectra of AISI 304 at RT ■, 200 °C ■ and 400 ° C ■: (a) outside the wear track, (b) inside the wear track.

IV. Conclusions

A functional test bench was successfully set up to replicate dry abrasion tests according to ASTM G-65, within a temperature range from RT to 400°C. This allowed for the evaluation of the effect of temperature on the wear of AISI 304 austenitic stainless steel.

Gravimetric results showed that the wear rate decreases with increasing temperature, moreover slight increase in hardness was observed on the surface of the specimens as the temperature increases in the tests. This behavior is attributed to the softening of stainless steel at high temperatures, which promotes plastic deformation and reduces material removal.

The microstructure of stainless steel is affected by its allotropic properties; it is well known that its mechanical strength and elasticity begin to be compromised above 315°C. In this context, the predominant wear mechanisms observed were plastic deformation, cracking, and plowing.

A transition in the wear mechanism at 400°C was confirmed by Raman spectroscopy, which revealed the growth of a thick and crystalline oxide layer composed of magnetite (Fe_3O_4) and iron-chromium spinels. This protective layer is a tribochemical product, formed when the combination of ambient heat, frictional flash temperatures, and plastic deformation provides the necessary activation energy to accelerate oxidation, effectively acting as a solid lubricant.

Científica, vol. 30, no. 1, pp. 01-12, January-June 2026,
ISSN 2594-2921, Instituto Politécnico Nacional, México
e300105 | DOI: 10.46842/ipn.cien.v30n1a05

CRediT (*Contributor Roles Taxonomy*)
Author Contributions: Conceptualization: JO**AV**; Methodology: JO**AV**; Investigation: ME**SH**, SI**TV**; Writing-original draft preparation: SI**TV**, FJ**AG**; Writing-review and editing: C**SR**, SI**TV**; Supervision: C**SR**; Formal analysis: C**SR**, SI**TV**.
Funding: This research received no external funding.
Data Availability Statement: The original contributions presented in this study are included in the article. Further inquiries can be directed to the corresponding author.
Acknowledgments: We recognize the experimental support of the laboratories of Machines-Tools and Welding of CUCSUR, Universidad de Guadalajara.
Conflicts of Interest: The authors declare no conflicts of interest.

REFERENCIAS

[1] J. A. Williams, "Wear and wear particles - Some fundamentals," *Tribol. Int.*, vol. 38, no. 10, pp. 863–870, Oct. 2005, doi: https://doi.org/10.1016/j.triboint.2005.03.007
[2] H. Dong, "Tribological properties of titanium-based alloys," in *Surface Engineering of Light Alloys: Aluminium, Magnesium and Titanium Alloys*, Elsevier Inc., 2010, pp. 58–80. doi: https://doi.org/10.1533/9781845699451.1.58
[3] E. Badisch, C. Katsich, H. Winkelmann, F. Franek, M. Roy, "Wear behaviour of hardfaced Fe-Cr-C alloy and austenitic steel under 2-body and 3-body conditions at elevated temperature," *Tribol. Int.*, vol. 43, no. 7, pp. 1234–1244, Jul. 2010, doi: https://doi.org/10.1016/j.triboint.2010.01.008
[4] S. Affatato, D. Brando, "Introduction to wear phenomena of orthopaedic implants," in *Wear of Orthopaedic Implants and Artificial Joints*, Elsevier, 2013, pp. 3–26. doi: https://doi.org/10.1533/9780857096128.1.3
[5] M. Cristina, M. Farías, D. K. Tanaka, A. Sinatora, M. E. Santos Taqueda, "Study of the Wear Behavior of AISI 304 Austenitic Stainless Steel Using Response Surface Methodology," *Proceedings of 17th International Congress of Mechanical Engineering*, Sao Paulo, Brasil, 2003. Available in: https://abcm.org.br/anais/cobem/2003/html/pdf/COB03-0871.pdf
[6] S. Hernandez, J. Hardell, C. Courbon, H. Winkelmann, B. Prakash, "High temperature friction and wear mechanism map for tool steel and boron steel tribopair," *Tribology - Materials, Surfaces and Interfaces*, vol. 8, no. 2, pp. 74–84, Jun. 2014, doi: https://doi.org/10.1179/1751584X13Y.0000000049
[7] L. C. Seabra, A. M. Baptista, "Tribological behaviour of food grade polymers against stainless steel in dry sliding and with sugar," *Wear*, vol. 253, no. 3-4, pp. 394-402, 2002, doi: https://doi.org/10.1016/S0043-1648(02)00138-2
[8] D. Odabas, "Effects of Load and Speed on Wear Rate of Abrasive Wear for 2014 Al Alloy," in *IOP Conference Series: Materials Science and Engineering, Institute of Physics Publishing*, Feb. 2018. doi: https://doi.org/10.1088/1757-899X/295/1/012008
[9] Y. Pei, D. Xia, S. Wang, L. Cong, X. Wang, and D. Wang, "Effects of temperature on the tribological properties of NM600 under sliding wear," *Materials*, vol. 12, no. 23, Dec. 2019, doi: https://doi.org/10.3390/ma12234009
[10] B. Passilly, A. Quelquejeu, and A. Kardache, "Mechanical properties of stainless steel by using high temperature microhardness tester," *Materiaux et Techniques*, vol. 111, no. 4, 2023, doi: https://doi.org/10.1051/mattech/2023021